Image quality with iterative reconstruction techniques in CT of the lungs—A phantom study

Hilde Kjernlie Andersen[a,*], David Völgyes[b], Anne Catrine Trægde Martinsen[a,c]

[a] Department of Diagnostic Physics, Oslo University Hospital, Oslo, Norway
[b] Faculty of Computer Science and Media Technology, Norwegian University of Science and Technology (NTNU), Gjøvik, Norway
[c] The Department of Physics, University in Oslo, Oslo, Norway

ABSTRACT

Background: Iterative reconstruction techniques for reducing radiation dose and improving image quality in CT have proved to work differently for different patient sizes, dose levels, and anatomical areas.
Purpose: This study aims to compare image quality in CT of the lungs between four high-end CT scanners using the recommended reconstruction techniques at different dose levels and patient sizes.
Material and methods: A lung phantom and an image quality phantom were scanned with four high-end scanners at fixed dose levels. Images were reconstructed with and without iterative reconstruction. Contrast-to-noise ratio, modulation transfer function, and peak frequency of the noise power spectrum were measured.
Results: IMR1 Sharp + and VEO improved contrast-to-noise ratio to a larger extent than the other iterative techniques, while maintaining spatial resolution. IMR1 Sharp + also maintained noise texture.
Conclusions: IMR1 Sharp + was the only reconstruction technique in this study which increased CNR to a large extent, while maintaining all other image quality parameters measured in this study.

1. Introduction

For decades, filtered back-projection (FBP) has been used in reconstruction of CT images. The FBP reconstruction technique is based on several assumptions that simplify CT geometry as a compromise between reconstruction speed and image noise [1,2]. FBP is fast, but inherently also adds noise to the images. Increased computer processing power and − cost have made other more complex reconstruction methods clinically feasible, and hence, CT vendors developed new methods for image reconstruction a decade ago. These techniques are aimed at reducing image noise and/or radiation dose [2–9]. One group of these techniques are statistical iterative reconstruction techniques or hybrid techniques, which are more demanding compared to FBP with respect to reconstruction time, but strives to reconstruct CT images with less noise than with FBP, while preserving details and edges [2,3,5,6]. The hybrid reconstruction techniques work both in projection space and in image space with iterations between them, and blends iterative and FBP reconstruction. The four hybrid reconstruction techniques assessed in this study were ASIR, AIDR3D, iDose and SAFIRE. Some vendors have also introduced model based iterative techniques, where object, scanner geometry and optics are modelled in addition to noise and photon statistics. Model-based iterative reconstruction techniques reduce noise and artifacts more than hybrid techniques, but may also alter image texture more. The two model based iterative techniques assessed in this study were VEO and IMR [1,4,7]. Iterative reconstruction techniques have also proved to work differently for different patient sizes, dose levels and anatomical areas [10,11], and in addition to noise reduction, these techniques also can potentially alter spatial resolution and image texture [12,13]. CT of the lungs is commonly used in frequent follow-up of cancer patients, and can potentially also be used for screening-purposes. Therefore, reconstruction techniques enabling low-dose examinations of the lungs are of great importance for the patient. The aim of this study was to compare quantitative image quality parameters in CT of the lungs for high-end CT scanners from GE, Philips, Siemens and Toshiba using the recommended reconstruction techniques at different dose levels and patient sizes.

2. Material and methods

2.1. Phantoms

The image quality phantom Catphan600® [14] and the Kyoto Kagaku Lungman® [15] lung phantom were scanned in this study. The lung phantom was a torso with soft tissue and bone, and inside the cavity, the phantom consisted of heart, trachea, pulmonary vessels and diaphragm/abdomen. The size of the phantom was 43 cm lateral diameter x 40 cm anteroposterior diameter, and 48 cm hight, with a circumference of 94 cm. The lung phantom was used both with and without additional padding, simulating a small and a large patient. With padding, 30 mm was added to the front and to the back of the phantom. The soft tissue and vessels of the lung phantom were made from polyurethane (gravity1.06), and the bone structures were made from epoxy resin and calcium carbonate. The lung phantom contained two spherical inserts of 12 mm in diameter simulating both high- and low-density lesions. The nominal densities of the lesions were approximately −800 and +100 HU. The Catphan600® is an image quality phantom for quantitative measurements. In this study, the module CTP528 for measurement of spatial resolution was used. The module consisted of two wolfram beads embedded in a homogenous material [14].

2.2. Image acquisition

The scanner models used were the Siemens Definition Flash®, Toshiba Aquilion ONE®, GE Discovery 750HD® and Philips Ingenuity®. Scan techniques and reconstruction techniques are given in detail in Tables 1 and 2. All scans were done with the clinical scan protocol for CT of the lungs for each scanner. Catphan600® was scanned with a fixed dose level of 10 mGy CTDIvol. For the lung phantom, fixed dose levels of 2.5 mGy, 5 mGy and 10 mGy CTDIvol were used. All images were reconstructed to the same thickness of 2 mm, in order for measurements to be comparable. Images were reconstructed using the filtered back-projection (FBP) techniques for CT of the lungs, and also with a selection of the iterative options available on the scanners. The reconstruction kernels and levels of iterative reconstruction used were chosen according to recommendations from the vendors. The hybrid iterative techniques are a blend between FBP and iterative reconstruction. All these are based on the kernel used for the FBP reconstruction. With respect to Philips' Iterative Model Reconstruction (IMR) and GE's Model-based iterative reconstruction (VEO), these are not kernel based, but stand-alone reconstruction algorithms.

Table 1
Scan technique for all scanners and both phantoms.

	GE	Siemens	Philips	Toshiba
Detector width [mm]	40	38,4	40	40
Detector Collimation	64 × 0.625	64 × 0.6	64 × 0.625	80 × 0.5
rotation time [s/ rotation]	0.5	0.5	0.5	0.5
pitch	0.984	1.2	1.015	1.1
mA	65/125/255	89/178/360	77/154/315	70/130/260
CTDIvol [mGy]	2.6/4.9/10	2.5/5/10.1	2.5/5/10.1	2.7/5/9.9
kVp	120	120	120	120
Reconstructed slice thickness [mm]	2	2	2	2
Displayed field-of-view [cm] for lung phantom	32	32	32	32
Displayed field-of-view [cm] for Catphan (MTF)	21	21	21	21

Table 2
Reconstruction techniques for all image series.

Scanner	Reconstruction	
GE	VEO	VEO
	Lung	ASIR20
		FBP
Siemens	70f	SAFIRE3
		FBP
Philips	IMR1	Routine Sharp +
	YB	iDose2
		FBP
Toshiba	FC56	AIDR3DSTD
		FBP(QDS)

2.3. Image quality analyses

Contrast-to-noise ratio (CNR) in all 66 series of the lung phantom was calculated from two simulated lesions of size 12 mm in diameter, with nominal densities of approximately −800 and +100 HU. CNR between the lesions was calculated using the following formula [16]:

$$CNR = \frac{2(HU_1 - HU_2)^2}{SD_1^2 + SD_2^2}$$

Where HU_1 and HU_2 are the Hounsfield numbers measured in the two nodules, and SD_1 and SD_2 are the corresponding standard deviations (Figs. 1 and 2). CNR is one of the most commonly used image quality descriptors in CT, and gives valuable input to the visibility of lung nodules [17].

Noise texture refers to correlations between adjacent pixel values that are manifest by the grainy appearance of CT images. These correlations are largely affected by the reconstruction technique used, and may influence the detectability of pathology [12]. Images with equal noise magnitude but different noise texture may not have the same image quality [13]. Noise texture and magnitude may be characterized in terms of the noise power spectrum (NPS). NPS was measured in the liver area of the lung phantom for all scan series of the lung phantom (Fig. 3).

NPS was calculated with a square ROI with a size of 80 mm x 80 mm, subdivided into 4 squares, and repeated in the three central slices in order to minimize noise in the measurement with ensemble
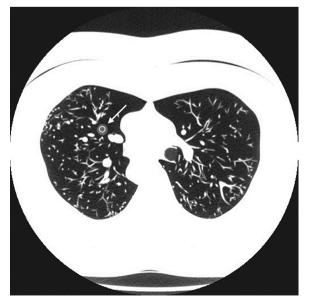

Fig. 1. Measurement of CNR in low-density insert simulating nodule.

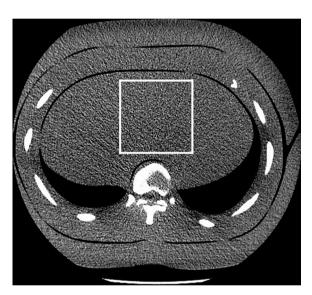Fig. 2. Measurement of CNR in high-density insert simulating nodule.

Fig. 3. Measurement of NPS in liver area of chest phantom.

averaging. A second order function was fitted and removed from the NPS to minimize beam hardening effect. The two-dimensional NPS [14] is proportional with the Fourier transformation (F) of the autocorrelation function of the signal, and was calculated as follows:

$$NPS(f_x, f_y) = c \times |F\{signal(x, y)\}|^2$$

Where f_x and f_y are the spatial frequencies in the x and y dimensions, $c = \frac{pixel\ size_x \times pixel\ size_y}{N_x \times N_y}$ and N_x and N_y are the pixel numbers in x and y directions.

The NPS can be expressed both in cartesian and polar coordinate system:

$$NPS(f_x, f_y) = NPS(r_f, \phi)r_f$$

Radial frequency is defined as: $r_f = \sqrt{f_x^2 + f_y^2}$, and the peak contributing frequency is the r_f radial frequency where the parenthesized expression reaches its maximum.

An in-house developed software was used for measurement and calculation of CNR and NPS.

Spatial resolution in measured in the module CTP528 of the Catphan600® image quality phantom for all series. The module contains

two wolfram beads embedded in a homogenous material. From these beads, the point-spread function was measured. The point-spread function describes the resolution in the spatial domain [18]. This function was transformed into the spatial-frequency domain, to obtain the modulation-transfer function (MTF) using the Fourier transform. The critical frequencies for 10% and 2% contrast were recorded using the commercially available software Image Owl [19].

3. Results

3.1. CNR

With respect to CNR, Toshiba measured higher values than the other vendors for both filtered back-projected images and the hybrid iterative techniques (range for both phantoms and all dose levels: Toshiba: 69-2180, the three others: 43-1819).

All scanners showed larger CNR with the use of iterative reconstruction techniques. In all but one case, the iterative techniques AIDR3Dstd (Toshiba) and SAFIRE3 (Siemens) compensated for dose reduction in such way that CNR was maintained or even improved using half the dose compared to filtered back-projection. Both ASIR20 (GE) and iDose2 (Philips), also improved CNR compared to FBP, but not to the same extent as AIDR3Dstd and SAFIRE3.

For the iterative techniques VEO (GE) and IMR1 (Philips), the CNR was higher than for all the other images, independent of manufacturer (range for all dose levels and both phantom sizes: 2546–44991 vs 43–2179 for the other techniques). The IMR1 Routine had the highest CNR for the highest dose levels with the small phantom, and was on the level of VEO for the series with lower dose or larger phantom. The IMR1 Sharp+ had an overall lower CNR than both VEO and IMR1 Routine.

CNR data is shown in Table 3.

3.2. NPS peak frequency

Siemens and Philips measured the highest NPS peak frequencies for FBP images (range for all dose levels and phantom sizes: 0.60–0.65 for both Siemens and Philips FBP), GE measured somewhat lower, and Toshiba had the lowest peak frequency, indicating a more coarse noise texture in the images (range for all dose levels and phantom sizes: 0.55–0.60 for GE and 0.48–0.50 for Toshiba).

There was little difference in peak frequency between the FBP images and the different hybrid iterative techniques, except for the Toshiba AIDR3Dstd, which had a lower peak frequency (range for all dose levels and both phantom sizes for AIDR3Dstd: 0.33–0.45) than the corresponding FBP reconstructions. This difference increased with dose reduction and with phantom size.

VEO had a lower NPS peak frequency than the IMR1 Sharp+, and also than the other GE images. The variation of peak frequency for different dose levels and phantom sizes was smaller than for IMR routine.

The images reconstructed with IMR1 Routine had lower peak frequencies compared to the FBP images from Philips, and the frequency dropped further down for the low dose images. The variation of peak frequency for IMR routine was larger than for both VEO and IMR sharp+. NPS peak frequency for IMR1 Sharp+ was on the level of the FBP reconstructed images from Philips, and the variation of peak frequency was smaller than for both VEO and IMR Sharp+ (range for all dose levels and both phantom sizes: VEO: 0.38–0.45, IMR routine: 0.33–0.50, IMR sharp+: 0.58–0.63). NPS peak frequency data is shown in Table 3.

3.3. MTF

For FBP reconstructions, Siemens and GE had the highest critical frequencies for 10% and 2% of MTF (Siemens: 10.6 and 12.2 cycles/cm, GE: 10.9 and 12.2 cycles/cm for 10% and 2% MTF, respectively).

Table 3
CNR, NPS peak frequency and MTF for all reconstructed series.

Dose level	Vendor	Algorithm/Kernel	Technique	CNR		NPS peak frequency		MTF critical frequency	
				Large	Small	Large	Small	10% contrast	2% contrast
10 mGy	GE	VEO	VEO	20272	26195	0.38	0.43	10.2	12.2
		Lung	ASIR20	360	1109	0.55	0.58	10.1	12.2
			FBP	281	820	0.60	0.58	10.9	12.2
	Siemens	70f	SAFIRE3	441	1819	0.65	0.63	9.8	10.6
			FBP	141	569	0.65	0.63	10.6	12.2
	Philips	IMR1	Routine	19555	44991	0.50	0.50	8.1	9.6
			Sharp+	6774	11063	0.58	0.60	10.2	11.4
		YB	iDose2	360	1567	0.65	0.63	10.1	11.3
			FBP	248	1084	0.65	0.63	10.2	11.4
	Toshiba	FC56	AIDR3DSTD	963	2180	0.43	0.45	8.8	10.5
			FBP	326	1233	0.50	0.50	8.9	10.1
5 mGy	GE	VEO	VEO	9750	17291	0.45	0.43		
		Lung	ASIR20	121	630	0.58	0.55		
			FBP	104	475	0.58	0.55		
	Siemens	70f	SAFIRE3	380	754	0.58	0.60		
			FBP	117	237	0.60	0.60		
	Philips	IMR1	Routine	8496	32425	0.45	0.50		
			Sharp+	3222	7652	0.60	0.63		
		YB	iDose2	94	569	0.60	0.63		
			FBP	65	393	0.60	0.63		
	Toshiba	FC56	AIDR3DSTD	636	1130	0.40	0.43		
			FBP	162	610	0.50	0.50		
2.5 mGy	GE	VEO	VEO	9480	10317	0.40	0.45		
		Lung	ASIR20	82	204	0.58	0.58		
			FBP	62	168	0.58	0.58		
	Siemens	70f	SAFIRE3	208	524	0.63	0.60		
			FBP	67	171	0.63	0.65		
	Philips	IMR1	Routine	5888	10257	0.33	0.35		
			Sharp+	2546	4127	0.60	0.58		
		YB	iDose2	66	194	0.60	0.60		
			FBP	43	134	0.65	0.60		
	Toshiba	FC56	AIDR3DSTD	316	887	0.33	0.40		
			FBP	69	337	0.48	0.48		

Philips measured somewhat lower (10.2 and 11.4 cycles/cm for 10% and 2% MTF, respectively), and Toshiba had the lowest critical frequencies (8.9 and 10.1 cycles/cm for 10% and 2% MTF, respectively).

With iterative reconstruction, iDose2 and AIDR3Dstd measured on the same level as FBP (iDose2: 10.1 and 11.3 cycles/cm, AIDR3Dstd: 8.8 and 10.5 cycles/cm for 10% and 2% MTF, respectively). Asir20 had a drop for 10% MTF compared to FBP, and SAFIRE3 had drop for both 10% MTF and 2% MTF with use of SAFIRE3 (Asir20: 10.1 and 12.2 cycles/cm, SAFIRE3: 9.8 and 10.6 cycles/cm for 10% and 2% MTF, respectively).

IMR1 Sharp+ measured similar MTF as the both the hybrid and the FBP images from Philips (10.2 and 11.4 cycles/cm for 10% and 2% MTF, respectively), while VEO (10.2 and 12.2 cycles/cm for 10% and 2% MTF, respectively) was on the same level as Asir20, and IMR1 Routine measured lower MTF (8.1 and 9.6 cycles/cm for 10% and 2% MTF, respectively) than both the hybrid and the FBP images from Philips, and also lower than VEO and IMR Sharp+. MTF data is shown in Table 3.

4. Discussion

The FC56 FBP reconstruction filter from Toshiba had the highest CNR and the lowest MTF and NPS peak frequency among the FBP images. This indicates that the recommended lung reconstruction filter FC56 for Toshiba is not as sharp as the other FBP reconstruction filters in this study, although the differences between vendors seen in this study, in addition to properties of the lung reconstruction filters, may also result from differences in scanner hardware.

All hybrid iterative techniques improved CNR. The iterative techniques reduced noise, but did not improve contrast to the same degree.

Hence, the improvement in CNR was mainly due to the noise reducing properties of the hybrid iterative techniques. AIDR3Dstd (Toshiba) and SAFIRE3 (Siemens) maintained or improved CNR using half the dose compared to FBP, while ASIR20 (GE) and iDose2 (Philips) did not compensate to the same extent. This may be due to the properties of the iterative reconstruction algorithms, and also the different levels of iterative reconstruction applied. These results comply with other studies on hybrid iterative reconstruction techniques in chest CT [20–24].

MTF is a descriptor of the spatial resolution in the image, and for CT examinations of the lung, the spatial resolution is one of the most important image quality properties. iDose2 and AIDR3Dstd maintained the MTF compared to the corresponding FBP images. ASIR20 had a drop for 10% MTF compared to FBP, and SAFIRE3 had a drop for both 2% and 10% MTF. The ability of the iterative reconstruction techniques to preserve spatial resolution in the images is critical when it comes to applicability of these techniques in CT of the lungs, and iDose2 and AIDR3Dstd proved advantageous in this respect.

A drop in peak frequency of the NPS reflects a shift to a more coarse noise texture in the image. This will affect the visual impression of the image, and thereby possibly also the diagnostic quality of the image [13]. All hybrid iterative techniques maintained NPS peak frequency except AIDR3Dstd, which had a drop in peak frequency compared to FBP reconstructions, increasing for lower doses and large phantom. Hence, AIDR3Dstd proved disadvantageous in this respect.

VEO and IMR1 largely improved CNR compared to FBP. This corresponds to other studies, who also found large noise reductions using VEO or IMR for chest CT [20,25,26]. With respect to MTF, VEO and IMR1 Sharp+ measured at the same level as the corresponding FBP lung reconstruction filters, while IMR1 Routine measured a lower MTF. With respect to NPS peak frequency, VEO and IMR1 Routine were on a

lower level than the FBP reconstructed images, and also lower than IMR1 Sharp +, indicating a more coarse noise texture. The IMR1 Sharp + measured similar peak frequency of the NPS as the corresponding FBP images, hence, both spatial resolution and noise texture was preserved using IMR1 Sharp +. The IMR1 Sharp + is dedicated for high resolution CT imaging, and these results indicate that this reconstruction technique emphasizes the properties important for these examinations.

IMR1 showed more variation between phantom sizes and dose levels than VEO. This indicates that these algorithms work differently with respect to aggressiveness in noise reduction depending on inherent noise in the signal.

Improvements in CNR from use of iterative reconstruction techniques in this study were resulting mainly from the noise reducing properties of the iterative techniques. The model based iterative techniques were more noise reducing than the hybrid techniques, and hence, these techniques were also the ones improving CNR the most in this study.

Noise texture can potentially affect diagnostic image quality and lesion detectability [13]. A shift in NPS compared to FBP results from a change in noise texture, and will affect the diagnostic image quality. The lower peak frequency for VEO, AIDR3Dstd and IMR1 Routine compared to the corresponding FBP techniques indicate such a shift, and could therefore potentially be unbeneficial in CT of the lungs.

In CT of the lungs, visualization of small structures like nodules and fine airway structures are of great importance. Hence, the preservation of edges and details is detrimental in the application of iterative reconstruction techniques in CT of the lungs. With respect to spatial resolution and MTF, the drop in MTF measured for SAFIRE3 and IMR1 Routine, and partially for ASIR20, could potentially degrade the visualization of small details, which would not be beneficial for CT of the lungs.

This study has limitations. The measurements of spatial resolution in this study were done by calculating the MTF from a high contrast point source, and as iterative reconstruction techniques are non-linear, these MTF measurements may not describe the total sharpness of the images. Still, in CT of the lungs, the sharpness of the small, high contrast details are of dominating importance, which is what is reflected in the measurements in this study.

In clinical practice, the visibility of smaller lesions is of greater importance than that of larger lesions. CNR was measured in large nodules of 12 mm in diameter to avoid partial volume effect. However, the CNR for larger lesions will in great part reflect also the CNR for smaller lesions.

The iterative reconstruction algorithms varied with respect to how much they compensated for dose reduction for the CNR measurements. Other strengths of iterative reconstruction could compensate differently for dose reduction, and would possibly also behave differently with respect to MTF and NPS. The scales of strength for the different algorithms are not comparable, and in this study the levels of iterative reconstruction recommended by the vendors were evaluated and compared. An evaluation of the whole range of iterative strengths could establish which levels are most comparable, but this was not the scope of this study.

Only quantitative image quality has been assessed in this study. Although the parameters measured in this study are important descriptors of image quality in CT of the lungs, diagnostic quality of the images should also be assessed in human observer analyses.

5. Conclusions

IMR1 Sharp + and VEO improved contrast-to-noise ratio to a larger extent than the other iterative techniques, while maintaining spatial resolution. IMR1 Sharp + also maintained noise texture, hence, this technique proved advantageous with respect to image quality for CT of the lungs.

References

[1] W.P. Shuman, D.E. Green, J.M. Busey, et al., Model-based iterative reconstruction versus adaptive statistical iterative reconstruction and filtered back projection in liver 64-MDCT: focal lesion detection, lesion conspicuity, and image noise, AJR 200 (2013) 1071–1076.

[2] S. Singh, A.K. Kalra, J. Hsieh, et al., Abdominal CT: comparison of adaptive statistical iterative and filtered back projection reconstruction techniques, Radiology 257 (2) (2010) 373–383.

[3] E. Angel, AIDR 3D Iterative Reconstruction (White Paper). Toshiba Medical Systems, (2012) (Accessed January 12, 2018) Available from: http://medical.toshiba.com/downloads/aidr-3d-wp-aidr-3d.

[4] GE Healthcare, Introducing Veo on Discovery CT750 HD—Great Care by Design (White Paper), General Electric Company, 2011 (Accessed January 12, 2018) Available from: http://www3.gehealthcare.com/sitecore%20modules/web/~/media/documents/turkey/products/computed%20tomography/brochures/discovery%20ct750%20freedom%20edition/discovery%20ct750%20hd%20veo.pdf.

[5] K. Grant, R. Raupach, SAFIRE: Sinogram Affirmed Iterative Reconstruction (White Paper), Siemens Healthcare, 2012 (Accessed January 12, 2018) Available from: http://imaging.ubmmedica.com/all/editorial/diagnosticimaging/pdfs/SAFIRE.pdf.

[6] A. Vlassenbroek, D. Mehta, J. Yanof, CT radiation dose: Philips perspective, in: D. Tack, M. Kalra, P. Gevenois (Eds.), Radiation Dose from Multidetector CT, Medical Radiology, Springer-Verlag, Berlin, Heidelberg, 2012, pp. 617–632.

[7] D. Mehta, R. Thompson, T. Morton, et al., Iterative model reconstruction: simultaneously lowered computed tomography radiation dose and improved image quality, Med. Phys. Int. 1 (2013) 147–155.

[8] M.J. Willemink, P.A. de Jong, T. Leiner, et al., Iterative techniques for computed tomography Part 1: technical principles, Eur. Radiol. 23 (2013) 1623–1631.

[9] M.J. Willemink, T. Leiner, P.A. de Jong, et al., Iterative techniques for computed tomography Part 2: initial results in dose reduction and image quality, Eur. Radiol. 23 (2013) 1632–1642.

[10] M. Patino, J.M. Fuentes, K. Hayano, et al., A quantitative comparison of noise reduction across five commercial (hybrid and model based) iterative reconstruction techniques: an anthropomorphic phantom study, AJR 214 (2015) 176–183.

[11] K. Jensen, A.C.T. Martinsen, A. Tingberg, et al., Comparing five different iterative reconstruction algorithms for computed tomography in an ROC study, Eur. Radiol. 24 (2014) 2989–3002.

[12] J.B. Solomon, O. Christianson, E. Samei, Quantitative comparison of noise texture across CT scanners from different manufacturers, Med. Phys. 39 (10) (2012) 6048–6055.

[13] K. Boedeker, V.N. Cooper, M.F. McNitt-Gray, Application of the noise power spectrum in modern diagnostic MDCT. Part I. Measurement of noise power spectra and noise equivalent quanta, Phys. Med. Biol. 52 (2007) 4027–4046.

[14] The Phantom Laboratory Catphan ® 500 and 600 Manual, (2018) (Accessed January 11, 2018) Available from: https://www.phantomlab.com/s/Catphan-500600-Manual.pdf.

[15] Kyoto Kagaku co LTD, Chest Phantom N1, Instruction Manual, (2016) (Accessed June 17, 2016) Available from: http://kyotokagaku.com/products/detail03/pdf/ph-1_manual.pdf.

[16] A. Thitaikumar, T.A. Krouskop, J. Ophir, Signal-to-noise ratio: contrast-to-noise ratio and their trade- offs with resolution in axial-shear strain elastography, Phys. Med. Biol. 52 (2007) 13–28.

[17] S.M. Hashemi, H. Mehrez, R.S.C. Cobbold, et al., Optimal image reconstruction for detection and characterization of small pulmonary nodules during low-dose CT, Eur. Radiol. 24 (2014) 1239–1250.

[18] International commission on radiation units and measurements ICRU report No. 87: radiation dose and image-quality assessment in computed tomography, J. ICRU 12 (2012) 121–134.

[19] Help.imageowl.com [internet] Greenwich, NY, USA: c2016 [cited 2017 Jan 04]. Available from: http://help.imageowl.com/index.php/Catphan%C2%AEQA_Reports_-_Data_Information#MTF_Plot_from_Beads.

[20] M. Katsura, I. Matsuda, M. Akahane, et al., Model-based iterative reconstruction technique for ultralow-dose chest CT: Comparison of pulmonary Nodule detectability with the Adaptive Statistical Iterative Reconstruction Technique, Invest. Radiol. 48 (2013) 206–212.

[21] A. Ploussi, E. Alexopoulou, N. Economopoulos, et al., Patient radiation exposure and image quality: evaluation with the use of iDose4 iterative reconstruction algorithm in chest abdomen-pelvis CT examinations, Radiat. Prot. Dosim. 158 (2014) 399–405.

[22] W.L. Yang, F.H. Yan, B.L. Liu, et al., Can Sinogram-affirmed iterative (SAFIRE)

reconstruction improve imaging quality on low-dose Lung CT screening compared with traditional filtered back projection (FBP) reconstruction, J. Comput. Assist. Tomogr. 37 (2013) 301–305.

[23] S. Seki, H. Koyama, Y. Ohno, et al., Adaptive iterative dose reduction 3D (AIDR 3D) vs. filtered back projection: radiation dose reduction capabilities of wide volume and helical scanning techniques on area-detector CT in a chest phantom study, Acta Radiol. 57 (2016) 684–690.

[24] Y. Yamada, M. Jinzaki, T. Hosokawa, et al., Dose reduction in chest CT: Comparison of the adaptive iterative dose reduction 3D, adaptive iterative dosereduction, and

filtered back projection reconstruction techniques, Eur. J. Radiol. 81 (2012) 4185–4195.

[25] H. Yuki, S. Oda, D. Utsunomiya, et al., Clinical impact of model-based type iterative reconstruction with fast reconstruction time on image quality of low-dose screening chest CT, Acta Radiol. 57 (2016) 295–302.

[26] K. Jensen, T.M. Aaloekken, A. Tingberg, et al., Image quality in oncologic chest computerized tomography with iterative reconstruction: a phantom study, J. Comput. Assist. Tomogr. 40 (2016) 351–356.